Elastic and Inelastic Scattering Enhanced Spherical and Rectangular Silicon Photodiodes in Amorphous and Crystalline Liquids

by

Muhammad Hamza Humayun

A Thesis Submitted to the
Graduate School of Sciences and Engineering
in Partial Fulfillment of the Requirements for
the Degree of

Master of Science
in
Optoelectronics and Photonics Engineering

Koç University

September 2015

Koç University

Graduate School of Sciences and Engineering

This is to certify that I have examined this copy of a master's thesis by

Muhammad Hamza Humayun

and have found that it is complete and satisfactory in all respects,

and that any and all revisions required by the final

examining committee have been made.

Committee Members:

_____

Ali Serpengüzel, Ph. D. (Advisor)

_____

Özgür Müstecaplıoğlu, Ph. D.

_____

Selçuk Aktürk, Ph. D.

Date: _____

Abstract

When light interacts with matter, absorption, scattering and fluorescence of light can take place depending on the wavelength and energy of the light together with the size of the interacting particle. In this work, we present light scattering enhancement of spherically shaped silicon photodetectors immersed in liquid environments. Our results indicate higher detection performance for spherical surface detectors as compared to conventional flat surface photodiodes. In order to characterize the photodiodes, we devised a measurement setup with a diode pumped solid state laser (DPSS) operating at 532 nm wavelength to induce light scattering in the liquid solutions. The solutions used were pure ethanol, 0.1 mM Rhodamine 640 perchlorate in ethanol, pure 5CB nematic liquid crystal, and 0.1 mM Rhodamine 640 perchlorate in 5CB, Rhodamine solution gives the ability of fluorescence in addition to the light scattering. We obtained elastic light scattering in ethanol and liquid crystal solutions and inelastic light scattering in fluorescent solutions with the laser dye. The silicon photodiodes were immersed in the solutions and characterized for their responsivity for the detection of scattering. Positional tomography for the voltage response of the photodetectors was recorded. It is seen that the flat photodetector responded as directional, whereas the sphere's responsivity pattern showed omnidirectional detection angle. Inelastic scattering, i.e. fluorescence increases the response. Elastic scattering by the LC also increases the response. Dye in LC has decreased response. Different solutions of laser dye in LC need to be studied for optimum performance. The results indicate higher performance for spherically shaped silicon photodetectors and these results can be applied to optics of highly scattering media.

Özet

Işık ve özdek birbiri ile etkileşimi sonucu ışığın soğurulması, saçılması, fotoışıma gibi olaylar ortaya çıkmaktadır. Bu etkileşimler ışığın dalgaboyu ile erkine bağlıyken aynı zamanda özdek parçacıklarının boyuna da bağlıdır. Bu çalışmada, ışığın saçılmasının incelenmesi için sıvı ortamında kullanılan silisyum ışık algılayıcılarda iyileştirme elde edilmesi amaçlanmıştır. Işık algılayıcıların elektriksel olarak incelenmesi amacıyla bir elektrik akım-gerilim düzeneği kurulmuştur. Bu düzenekte çeşitli özelliklerde sıvı ortamlarının yer aldığı bir küvet ve sıvıların uyarılması için 532 nm dalgaboyunda çalışan diyot uyarımlı katı durum lazeri ile birlikte ışık saçılması incelenmesi için ışık algılayıcıları kullanılmıştır. Kullanılan sıvılar, saf etanol, saf 5CB nematik evredeki sıvı örüt, ve bunların 0.1 mM rodamin 640 perklorat lazer boyası çözeltilerinden oluşmaktadır. Yapılan deneyler sonucunda sıvı örüt ve lazer boyası çözeltisinde elastik olmayan ışık saçılımı ve fotoışıma gözlemlenmiştir. Düz yüzeyli ve yuvarlak yüzeyli ışık algılayıcılarının sıvılar içerisindeki elektriksel yanıtları konuma bağlı dilimçizim kullanarak ölçülmüştür. Sonuçlara göre yuvarlak yüzeyli ışık algılayıcılarının, düz yüzeyli ışık algılayıcılarına göre sıvı ortamda daha iyi başarımlı olduğu görülmüştür. Elastik olmayan fotoışıma ışık algılayıcılarının derinlik algılamasını arttırmaktadır. Elastik saçılma sıvı örütlerde ışık algılamasını arttırmaktadır. En iyi algılama için sıvı örütte lazer boyasının derişimini incelemek gerekecektir. Elde edilen sonuçların ışığın saçılması ile uğraşan optik ve fotonik alanlarına yararlı olacağı öngörülmüştür.

Acknowledgements

I would like to express my gratitude to my advisor Professor Dr. Ali Serpengüzel for giving me the opportunity to work with him, his guidance and the experiences I earned throughout my two years working in the Koç University Microphotonics Research Laboratory. I would also like to thank my thesis committee members, Prof. Dr. Özgür Müstecaplıoğlu and Assoc. Prof. Dr. Selçuk Aktürk, for their valuable comments and helpful discussions which contributed to my thesis.

I would also like to thank research group members namely our postdoctoral research associate Dr. Ulaş Sabahattin Gökay, as he was very helpful during my stay here, Muhammad Sohail Anwar (MSc), Muhammad Rehan Chaudhry (MSc), Imran Khan (MSc), Zeeshan Rashid (PhD), Farhan Azeem Afridi (MSc), and especially my team members, Syed Sultan Shah Bukhari (MSc) and Muhammad Zakwan (PhD) for their help in building experimental setup and helping me with my thesis. It was really an honor to part of such wonderful team. I would also like to thank Selçuk Çakmak from Koç University Physics Department, Haris Sheh Zad from Manufacturing and Automation Research Center (MARC), Mehdi Aas from Optofluidics and Nano-Optics Laboratory, and Haroon Qureshi from Proteomics Laboratory, and Meisam Farzalipour Tabriz from Koç University program of Material Science & Engineering for their contribution and help in the research.

I would also like to thank Koç University Surface Science and Technology Research Center (KUYTAM) for their support. I would like to thank Kyosemi Corporation and Sphelar Power Corporation for the Sphelar ® sphere.

I would also like to acknowledge Türkiye Bilimsel ve Teknolojik Araştırma Kurumu (TÜBİTAK) grant No: 114F312 for the partial financial support to our research. Also I would thank Pakistan Higher Education Commission (HEC) for the financial support, which enabled me to come here in Turkey for graduate studies.

Finally, I would like to thank my family, especially my parents and my grandfather, to whom I dedicate this thesis, for encouraging me to pursue my education ambitions abroad.

Table of Contents

List of Figures

List of Tables

Chapter 1

INTRODUCTION

1.1 Light

Light is an electromagnetic wave, where visible light is generally considered portion of electromagnetic spectrum that humans can see and extends usually from ultraviolet range to far – infrared region. Optics is the branch of physics, in which we study the nature of light, where we study light's interaction with matter and the tools required to detect it [2].

Since the start of modern science, there has been a debate over whether light is a wave or particle. Newton held light having a particle nature, while Huygens was the exponent of light having wave nature. By 19th century, light having wave nature was widely accepted. In 1860s, James Maxwell unified phenomenon related to waves and developed electromagnetic theory of light, which are known as set of four Maxwell's equations, which in source free, free space are defined as [9]:

$$\nabla . E(r,t) = 0 \quad (1.1a),$$

$$\nabla . H(r,t) = 0 \quad (1.1b),$$

$$\nabla \times E(r,t) = -\mu_o \frac{\partial}{\partial t} H(r,t) \quad (1.1c),$$

$$\nabla \times H(r,t) = \varepsilon_o \frac{\partial}{\partial t} E(r,t) \quad (1.1d),$$

where $E(r,t)$ and $H(r,t)$ are electric field and magnetic fields, $\varepsilon_o = (1/36\pi) \times 10^{-9}$ (MKS units) the electric permittivity of free space, and $\mu_o = 4\pi \times 10^{-7}$ (MKS units) the magnetic permeability of free space.

Some of the phenomenon cannot be explained with classical theory; in such cases light behaves as both particle and wave, and 1900s saw the advent of quantum mechanics, which explains such phenomenon [5]. Max Planck led the way by solving the black body radiation problem of ultraviolet catastrophe by taking light as energy packets called photons. To summarize, light in nature exhibits wave-particle duality.

1.2 Photodetector

Study of light sensors is an important part of optics. Photodetector is a device, which provides a measurable physical response, when light is incident on it. The simplest example of light detector from nature is an eye [4]. In this thesis, our interest is in semiconductor solid state detectors. When light falls on these photodetectors, it excites electrons from valence band to conduction band, leaving behind holes in their place in the valence band. Electron hole pairs generated this way are called photogenerated carriers. The objective of the photodetector is to produce photocurrent in response to these photogenerated carriers in the external circuit. Each of the semiconductor compounds respond to different range of electromagnetic spectrum where bandgap energy of the semiconductor defines the window of responsivity [7]. In this case, the types of semiconductors can be given as intrinsic and extrinsic.

Photodiodes are extrinsic semiconductor devices with a built in p-n junction. The characteristic of the p-n junction is that, there are no free carriers in it, due to this the junction region is also called

depleted region, and there exists an electric field across it. The junction electric field is vital for separating the holes and electrons created due to light in the depleted region. By biasing the diodes, we can increase or decrease the electric field in the region. By reverse biasing, we can increase this electric field, and photodiode is said to be operating in photoconductive mode [8]. There are different parameters, on which the photodiodes are compared to each other, which basically compare how well the device collects those electron hole pairs generated [12].

For the photodetectors to work, the sensor must be able to absorb the light. When light interacts with matter, it can respond in various ways. It can scatter, and the type of scattering is dependent on the ratio of wavelength to the particle size. The scattering of light resulting with wavelength conserved is called elastic scattering, where Rayleigh and Mie scattering are the main examples [15]. If the wavelength is changed during the interaction, then it is called inelastic light scattering, where Raman scattering and fluorescence are the main examples [20]. The intensity of scattering will depend on the nature of medium. If the medium is non homogeneous, strongly polarizable, scattering would be intense [29]. If the medium is homogenous, then there will be less scattering. Scattering will be always there, when there is change of refractive index [26]. Here in this work, we are interested in photodetection of the elastic and inelastic scattered light. Following are the list of chapters and their content:

In Chapter 2, subject of photodetectors is discussed. We start with the physics of semiconductors, discuss how photodiode works, and conclude the chapter with performance parameters and simple circuit model of photodetector.

Chapter 3 is reserved for the light matter interaction. We discuss the interaction starting from the elastic light scattering from a single particle and then we move on to the light matter interactions

in fluidic medium. Then we discuss the inelastic light scattering, using the example of fluorescence. Absorption is also discussed as well. This chapter is concluded with, how absorption is affected by the presence of a scattering medium.

Chapter 4 is related to the experiment and the results. We introduce the photodiodes we used, their I-V characteristics, our experimental setup, results and conclude it by discussing our results.

Chapter 5 is the overall summary of the results and the analysis together with the possible applications.

Chapter 2

PHOTODETECTORS

Light is an electromagnetic radiation, which exhibits wave particle duality. It behaves as a wave while crossing the boundary between two objects and acts as a particle, while interacting with matter, for example photoelectric effect [1]. Electromagnetic radiation covers a wide range of wavelengths (or frequencies) and energies, usually expressed as electromagnetic spectrum. Wavelength (λ) and frequency (ν) are related through the velocity of the light (c) in space:

$$\lambda = cT = c / \upsilon \qquad (2.1),$$

In free space the light velocity, c, is constant and equal to 3×10^8 ms^{-1}. We would be restricting ourselves to optical window of the electromagnetic spectrum, which is usually taken from ultraviolet to far infrared range. Table 2.1 provides the wavelengths for the ranges covered in the optical window [2].

A photodetector is a solid state sensor used for the detection of light. It is used for conversion of light energy into electrical energy. Generally, photodetection comprises three steps: (1) absorption of the incident light followed by photogenerated charge carriers, (2) transportation of these carriers with or without current gain. In this process, the photogenerated carriers are moved across the absorption region, and (3) current interaction with external circuitry to provide output photocurrent [3]. There are two main types of photodetectors [4], (a) thermal detectors, and (b) quantum detectors.

Thermal detectors respond to incident light by changing temperature. Quantum detectors utilize the particle nature of light and respond to the rate of incident photons on the detector. Photons are also called light quanta. Albert Einstein suggested that electromagnetic field was quantized and consisted of corpuscles called photons. These photons travel at speed of light and have energy given by [5]:

$$E = h\nu = hc/\lambda \qquad (2.2),$$

where h is the Planck's constant 6.62618 x 10^{-34} Js.

Wavelength Range	Classification	Abbreviation
25 - 200 nm	Vacuum ultraviolet	VUV
200 - 400 nm	Ultraviolet	UV
400 - 700 nm	Visible	VIS
700 - 1000 nm	Near – Infrared	NIR
1 - 3 μm	Short-wavelength infrared	SWIR
3 – 5 μm	Medium-wavelength infrared	MWIR
5 – 14 μm	Long-wavelength infrared	LWIR
14 – 30 μm	Very long-wavelength infrared	VLWIR
30 – 100 μm	Far-infrared	FIR
100 – 1000 μm	Submillimeter	Sub MM

Table 2.1: The optical window.

The various quantum detectors are: (a) photovoltaic, (b) photoconductive, (c) photoemissive - photomultiplier tubes (PMTs), (d) photographic, (e) photoelectromagnetic, and (f) photoionization.

Photovoltaic cells also known as solar cells produce voltage, when illuminated by light. The most common example is PN junction type. When operated under bias condition, the mode of operation is termed as photoconductive mode of operation. Photodiodes can be operated in both photovoltaic mode and photoconductive mode. However, design of a solar cell is fundamentally different from that of a photodiode. Our focus in this research is on photoconductive detectors, and the remaining chapter would be dedicated to the theory, principle of operation, and parameters of photoconductive detector.

2.1 Energy Bands in Semiconductors

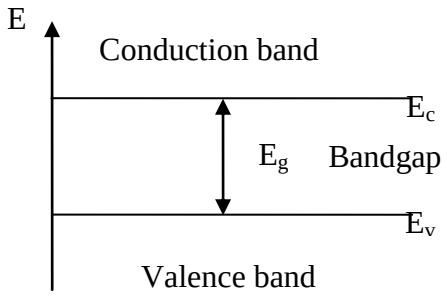

Figure 2.1: Band diagram of a semiconductor.

Electrons in a single atom can only have discrete energy levels, but when atoms are brought together like in crystalline solids, atomic interaction results in the splitting of these energy levels into many separate levels [6]. These energy levels are very closely spaced so that, they can be treated as a continuous band of allowed energy states. The two highest energy bands in the solids

are the valence band and the conduction band. These bands are separated by a region of energies, which electrons cannot possess. This region is called the bandgap (Fig. 2.1). The band gap energy (E_g) is the difference of energies of conduction band (E_c) and valence band (E_v).

Material	E_g (eV)	λ_{cutoff} (nm)	Spectral Band
Silicon	1.12	1100	VIS
Gallium Arsenide	1.42	875	VIS
Germanium	0.66	1800	NIR
Indium Gallium Arsenide*	0.73 – 0.47	1700 – 2600	NIR
Indium Arsenide	0.36	3400	NIR
Indium Antimonide	0.17	5700	MIR
Mercury Cadmium	0.7 – 0.1	1700 - 12500	Near to far IR
*The alloy composition of Indium Gallium Arsenide and Mercury Cadmium Telluride can be changed to alter the bandgap (E_g).			

Table 2.2: Photodetector materials.

Semiconductor photodetectors are fabricated from various materials. Each material has distinctive gap energy. E_g determines the light absorbing range of the material. Cutoff wavelength, λ_{cutoff}, is the wavelength, where photon energy is just enough for transition of electrons across band gap. The equation between the cutoff wavelength λ_{cutoff} and bandgap energy E_g is given by:

$$\lambda_{cutoff} = \frac{1.24x10^{3}\,nm}{E_g(eV)} \quad (2.3),$$

Table 2.2 gives band gap energy and cutoff wavelengths of widely used photodetector materials.

2.2 Photoconductor Principle of Operation

A photoconductor is made up of a slab of semiconductor with Ohmic contacts attached at the opposite ends to connect to the external circuit (Fig. 2.2).

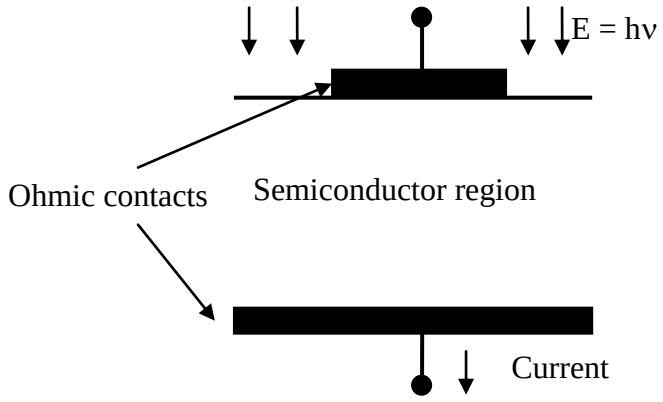

Figure 2.2: Photoconductor device diagram.

When light is incident on the photodetector, it excites the electrons within the atoms. If energy of the incident light is greater than bandgap energy, then the electron will leave the atom and jump to conduction band, and become a free electron leaving behind hole in the valence band. This electron is called photoexcited (Fig. 2.3). When an electron loses energy, it can fall back to the valence band, and fill a hole; this process is called recombination. There are two types of carrier transitions, when a semiconductor is excited: Intrinsic transition takes place, when carriers jump from band to band, and extrinsic transitions, when forbidden energy levels are also involved.

These intrinsic and extrinsic transitions result in an increase in conductivity. All the wavelengths shorter than the cutoff wavelength, λ_{cutoff} are absorbed by the detector [7].

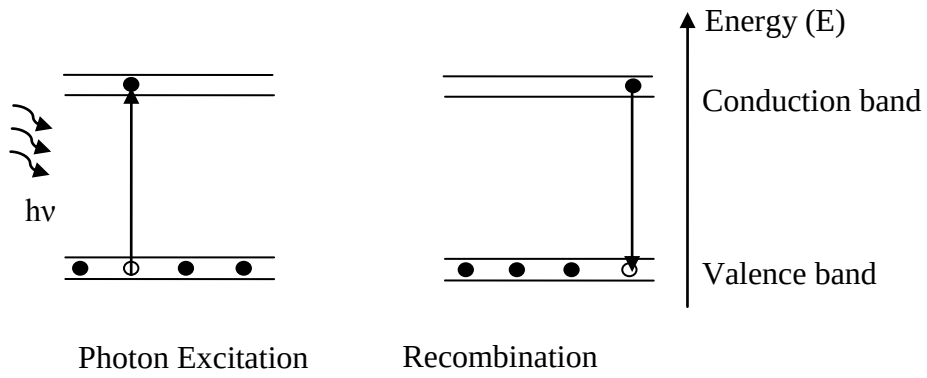

Figure 2.3: Photon excitation and recombination processes in semiconductors.

The photoconductor acts as a switch. When illuminated, it acts as close circuit, and when in dark it acts as open switch (Fig. 2.4).

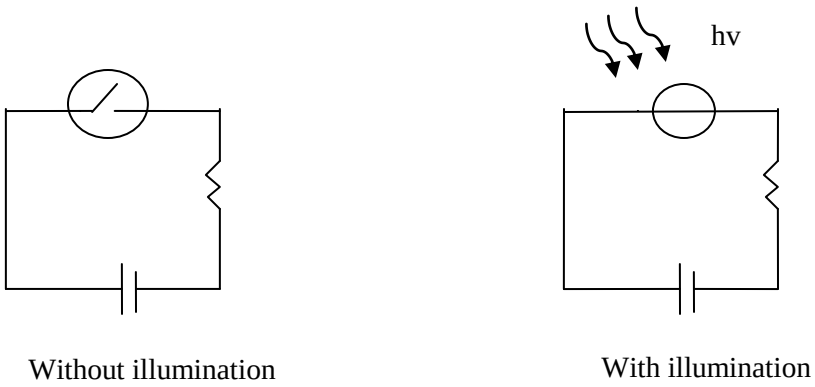

Figure 2.4 : Illumination effects on a photoconductor.

2.3 Photodiode

Photodiodes are semiconductor devices with a p-n junction. This junction is depleted of charged carriers hence is also called the depletion region. There is an electric field, which exists across the p-n junction. This electric field separates the electron-hole pairs (EHPs) generated due to incident light and they drift in opposite directions (Fig. 2.5): holes towards p-side and electrons towards n side. This drift current is in reverse direction to current in a simple diode. Next to depletion region, there are diffusion regions, where these photogenerated holes and electrons, minority carriers in those regions, can diffuse to the depletion layer, and then drift under the electric field. Beyond these diffusion regions, there is no current generated as there is no field to separate the photogenerated carriers, and these regions are termed as homogeneous sides (P or N). The minority carriers generated there recombine with the majority carriers. The area of depletion layer and the diffusion region on p and n side is called active region [8].

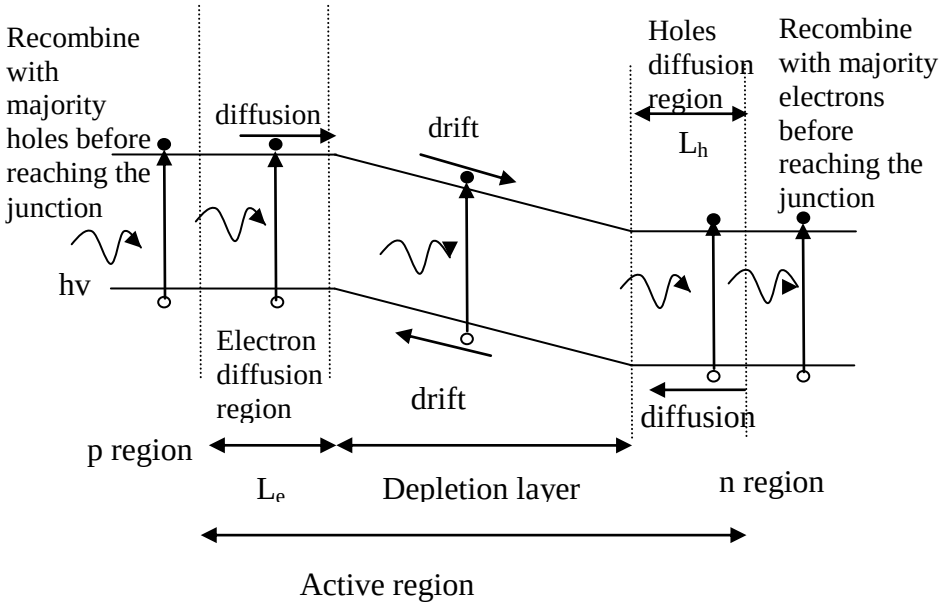

Figure 2.5: Energy band diagram of an unbiased p-n photodiode.

Let us suppose that a junction of cross-sectional area A is illuminated by photons having greater energy then the material's band gap energy. Also assume that illumination is uniform. This will result in photogeneration of carriers. If the rate of photogeneration is G (EHP/cm^3s), photocurrent will start to flow. The number of holes created per second within a diffusion length L_h of the depletion region on the n side is AL_HG. The number of electrons created per second within a diffusion length L_e of the depletion region on the p side is AL_eG. Similarly, AWG carriers would be generated within the depletion region of width W. The resulting junction photocurrent would be:

$$I_p = eA(L_h + L_e + W)G \quad (2.4),$$

The diode equation is given by:

$$I = I_0\left(e^{(eV/k_BT)} - 1\right) \quad (2.5),$$

where I_0 is the saturation current representing dark current. Therefore, the photodiode (PD) I-V characteristic equation would be:

$$I = I_0\left(e^{(eV/k_BT)} - 1\right) - I_p \quad (2.6),$$

where I_p would depend on intensity of the incident light [9].

2.4 Open Circuit Voltage (V_{oc}) and Short Circuit Current (I_{sc})

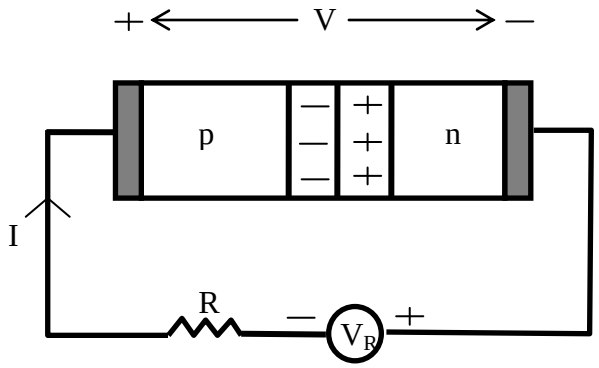

Figure 2.6: Biased PN junction diode.

The external battery is connected such that the PN junction is reverse biased to increase the electric field in the depletion region (Fig. 2.6). The current I in the circuit is given by Eq. 2.6. Using Kirchhoff's voltage law (KVL) in the circuit we get:

$$IR + V + V_R = 0 \qquad (2.7),$$

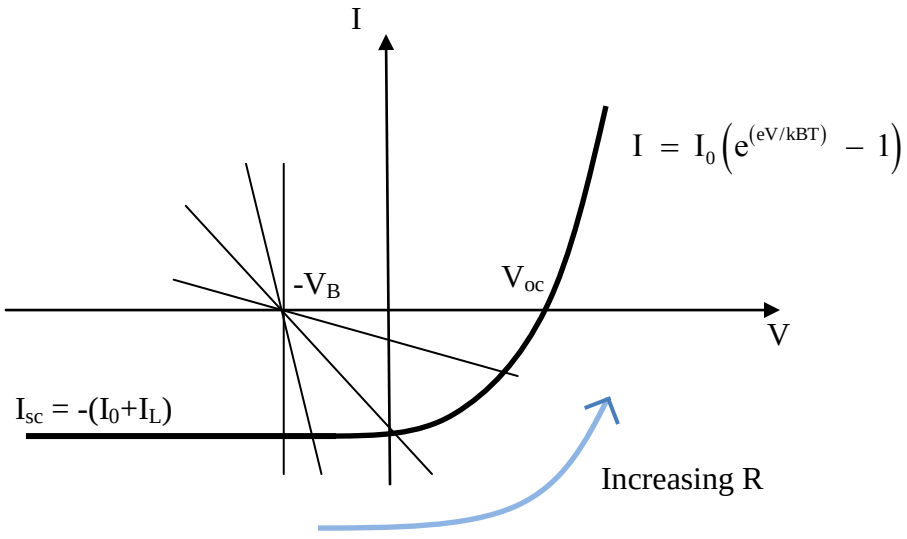

Figure 2.7: IV characteristic curve intersection with load line

The graphical solution of Eq. 2.6 and Eq. 2.7 is given in Fig. 2.7. Eq. 2.7 is called the load line and is drawn showing its increasing trend (Fig. 2.7).

In the ideal scenario, when R=0, and the junction is reverse biased, the current flowing in the circuit has of two parts; the current I_L due to photogeneration and the current I_o due to the reverse biased p-n junction. I_o is also called the 'dark' current of the photodetector, since it will be present even in the absence of light. This dark current is due to electron-hole generation in a reverse biased p-n diode and is unwanted.

When R = 0, the current flowing in the circuit is called the short circuit current and is given as:

$$I_{sc} = -(I_L + I_0) \tag{2.8}.$$

When R is made ∞, the voltage of the detector is called open circuit voltage and from Eq.2.6 it can be found as:

$$V_{oc} = \frac{KT}{q} \ln\left(\frac{I_l}{I_o} + 1\right) \tag{2.9}.$$

The symbol of the photodiode is given in (Fig. 2.8).

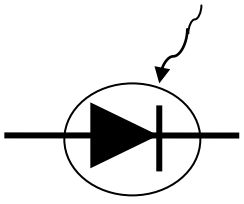

Figure 2.8: Photodiode symbol.

2.5 Photoconductive mode vs. photovoltaic mode

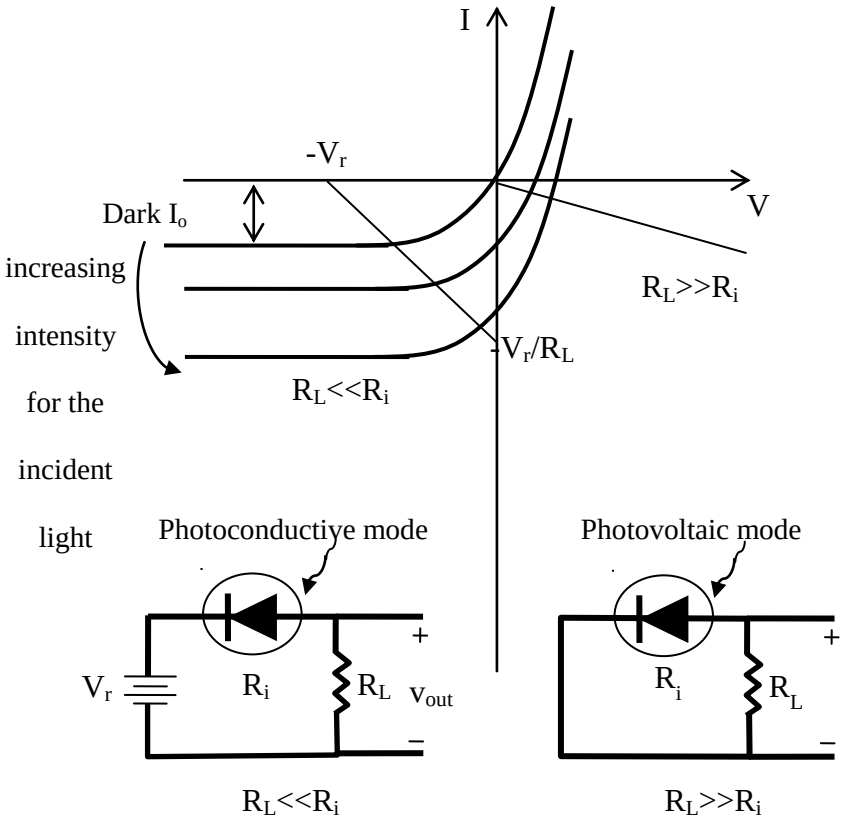

Figure 2.9: Photoconductive mode versus the photovoltaic mode of operation.

As stated earlier, the photodiode can be operated in photovoltaic mode, in which the photodiode is connected to a load resistance, and that is how a solar cell works. The photodiode is usually operated in reverse biased mode [10]. This reverse bias is not as high as to cause avalanche breakdown. The reverse biasing is beneficial for decreasing the carrier transit time and the diode capacitance [7] [11].

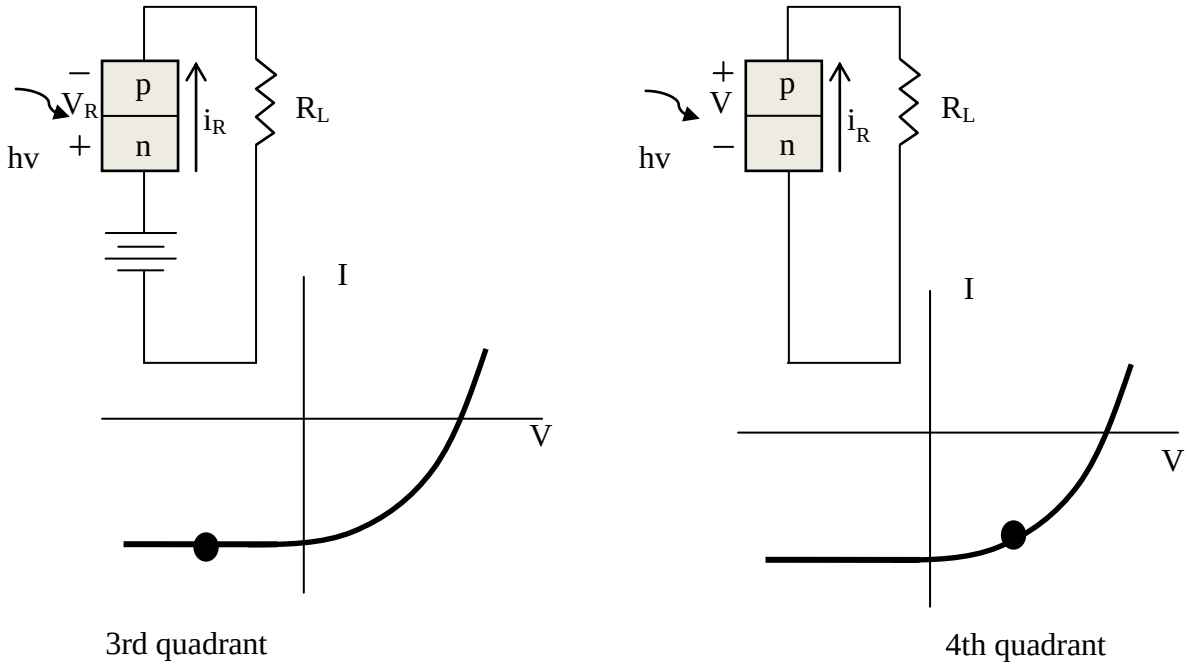

3rd quadrant

(external reverse bias, reverse current)

Photoconductive:

Power is delivered to

the device by the external

4th quadrant

(internal forward bias, reverse current)

Photovoltaic:

Power is delivered to

the load by the device

Figure 2.10: Comparison of the photoconductive and the photovoltaic mode of operations.

Fig. 2.9 graphically shows the difference between the two modes. In photoconductive mode, the output voltage (V_{out}) should be kept smaller than the biasing voltage (V_r) in order to keep the photodiode in reverse bias. This condition is met by keeping the load resistance (R_L) smaller than the internal resistance of photodiode (R_i) and keeping the biasing voltage large. In photovoltaic mode, the biasing voltage is not used, and the load resistance has to be large compared to the internal resistance of the photodiode. In this mode therefore the photovoltage forward biases the

photodiode. The operating point of photoconductive mode lies in the 3rd quadrant of I-V characteristic curve of photodiode, and the 4th quadrant for photovoltaic mode. This is summarized in Fig. 2.10.

2.6 Equivalent circuit of a Photodiode

The equivalent circuit of photodiode is shown in Fig. 2.11 [12]. In the figure, the current source represents the photogenerated current (I_L). This current varies proportionally to the incident photons. The diode represents the p-n junction. Photodiode has an internal resistance R_{sh} across its junction as well as a junction capacitance, C_j. The boundaries of the depletion region act like the plates of a parallel plate capacitor.

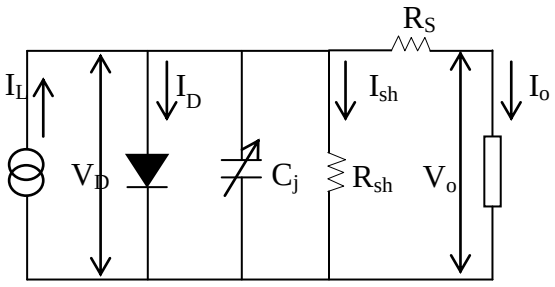

I_L: photogenerated current

V_D: voltage across diode

I_D: diode current

C_j: junction capacitance

R_{sh}: shunt resistance

R_S: series resistance

V_o: output voltage

I_o: output current

Figure 2.11: Equivalent circuit for a photodiode.

The junction capacitance is directly proportional to the diffusion area and inversely proportional to the width of the depletion region. R_{sh} and C_j depend on the size of photodiode, and their values vary with voltage across the junction. Internal resistance increases with increasing voltage,

however due to increased width of the depletion layer with the reverse voltage, the junction capacitance decreases. The series resistance R_S denotes both the resistance in the homogeneous regions of the diode and the parasitic resistance from the contacts.

2.7 Figures of Merit for the Photodiode

Key performance comparing parameters for photodetectors are quantum efficiency, responsivity, and response time.

2.7.1 Quantum Efficiency

Not all light, which is incident on the photodetector produces photocurrent. Some of the light is reflected off the surface. Some of the electron hole pair is recombined in the homogeneous region. Some photons are not absorbed by the photodetector; keeping in mind that the absorption process is probabilistic in nature. The quantum Efficiency, η, is the measure of the fraction of photons, that result in the flow of a photocurrent [9]:

$$\eta = (1 - R)\zeta(1 - e^{-\alpha d}) \qquad (2.10),$$

where R is the optical power reflectance at the surface, ζ the fraction of electron-hole pairs, that contribute to the detector current, α the absorption coefficient of the material (unit: m^{-1}), and d the photodetector depth. The quantum efficiency depends on the wavelength of the incident light. The dependence is represented in the absorption coefficient of Eq. 2.10.

2.7.2 Responsivity

The responsivity R(λ) is the ratio of photocurrent generated to the power of incident light at that wavelength.

$$R(\lambda) = \frac{I_{photogenerated}}{P} \quad (2.11).$$

The responsivity R(λ) can be defined in terms of quantum efficiency as:

$$R(\lambda) = \frac{\eta e}{h\nu} = \eta \frac{\lambda}{1.24} \quad (2.12).$$

The unit for R(λ) is (A/W), for λ in (μm), $h = 6.626 \times 10^{-34}$ Js is the Planck's constant, and $e = 1.602 \times 10^{-19}$ C is the unit charge.

2.7.3 Response Time

The response time is the measure of time taken by the photodetector to change in the incident light. The response time is affected by two processes, drift of electron and holes in the depletion layer, which is a fast process, and diffusion of electron hole pair in the diffusion regions, which is a slow process. Time taken for the fast process is called transit time. It is also dependent on the time constant τ = RC of the circuit. The resistance and capacitance are both from the photodiode and the external circuit [9].

Reducing the depletion region width makes the response of the photodiode fast, as the transit time is lessened. However, for higher quantum efficiency, the depletion region should be wider for more light capturing, so there is a tradeoff between quantum efficiency and response speed of the photodiode [7][13] .

Chapter 3

LIGHT MATTER INTERACTION

Matter has effect on light. Sky appearing blue, light scattering off the walls, transparency of water, and green foliage, in general, phenomenon like refraction, fluorescence and diffraction are some manifestations of the light matter interaction.

In this work, we are concerned with the phenomenon of absorption, elastic light scattering, and fluorescence. Fig. 3.1 gives the brief summary of various phenomena occurring due to light matter interaction.

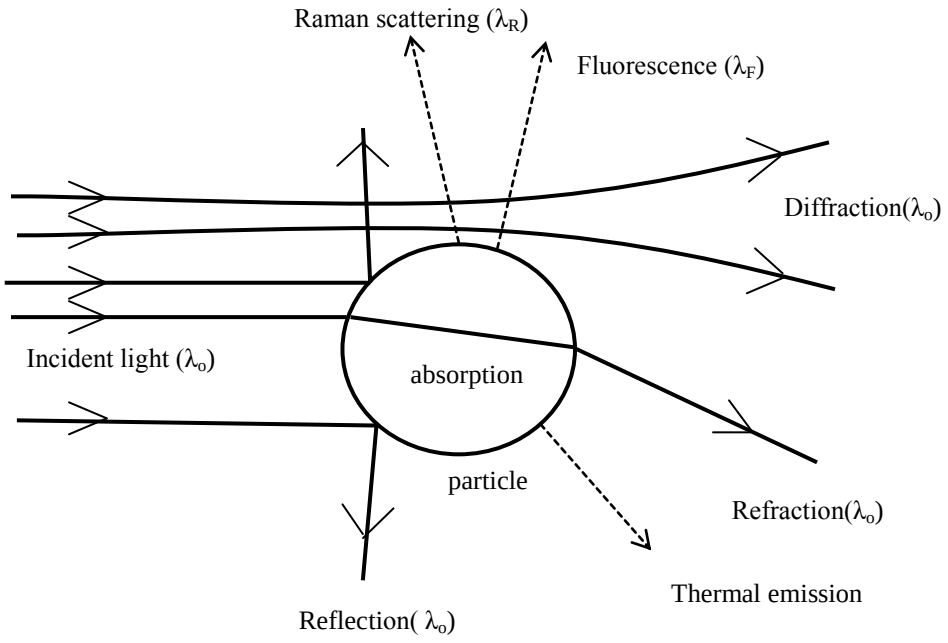

Figure 3.1: Light matter interaction mechanisms.

All objects' colors are determined by the way that light scatters off of them. The outcome of these interactions is dependent on the structure of matter as well as wavelength of the light [14]. So what is the reason for this interaction? Matter is made of positively charged nuclei surrounded by negative charged electrons, i.e., charge carriers. Moving charges as a result create localized electromagnetic field. Light itself is electromagnetic field with a certain frequency associated with it. When the light is incident on matter, the electric field of the electromagnetic wave cause the charged particles to start to oscillate, these oscillating charges then radiate electromagnetic field of their own. So what happens is that light's electric field applies accelerating force to the charged electrons and these accelerating electrons emit electromagnetic wave. This secondary emission is termed as scattering by that illuminated object (Fig. 3.2) [15] [16].

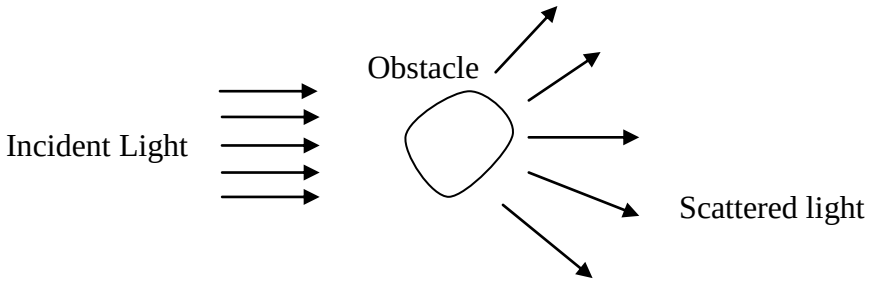

Figure 3.2: Light scattering by an obstacle.

Besides scattering, part of the incident light may be converted to other forms like thermal energy; this process is termed as absorption. So in scattering light is absorbed and reemitted, there is no change in energy of the emitted energy from the absorbed, hence no change in wavelength of the emitted light. There are cases, where there is change in wavelength and will be discussed in inelastic scattering. In absorption, the absorbed light results in a transition of an atom to a higher energy state. This energy produces vibrations in the material. Photon's energy produces heat in

this case. Fluorescence is the emission of light by matter after absorbing light. The light emitted has less energy than the absorbed light.

3.1 Light Scattering

Light scattering can be categorized as (a) elastic light scattering and (b) inelastic light scattering.

3.1.1 Elastic Light Scattering

As the electromagnetic (EM) wave encounters the obstacle or heterogeneity in the medium, it interacts with the discrete particles, the electron orbiting the particle's atoms are perturbed and set into oscillations with the same frequency as the electric field of the incident wave. The oscillation of the electron cloud results in a periodic separation of charges within the molecule thus inducing a dipole moment. The oscillating induced dipole moment acts as a source of EM radiation, this secondary emission is called the scattered light. The majority of light scattered by the particle is emitted at the same frequency of the incident light, a process called elastic scattering (Fig. 3.3).

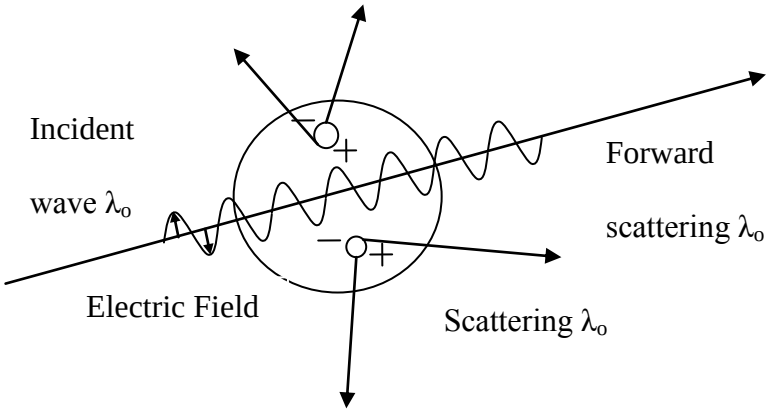

Figure 3.3: Scattering of light by an induced dipole.

The relationship between the wavelength of light and the size of obstacle is defined by the size parameter and is taken as:

$$x = \frac{2\pi a}{\lambda} = \frac{2\pi a N_o}{\lambda_o} \quad (3.1),$$

where a is the radius of particle, and λ the wavelength defined as λ_o/N_o , where N_o is the refractive index of surrounding medium, and λ_o the wavelength in vacuum.

According to the size parameter, the elastic scattering is taken as (a) Rayleigh scattering and (b) Mie scattering.

Rayleigh scattering theory is applied to the interaction of light with the particles having size parameters smaller than the incident light's wavelength, such as spherical, dielectric and non-absorbing particles. Mie scattering theory is applied with no limitation on the size of the absorbing or non-absorbing particle. For large particles, Mie scattering theory converges to the geometric optics limit. Mie theory can even be used for Rayleigh scattering systems. However, Mie scattering formulation is complex, so Rayleigh scattering theory is usually preferred, if applicable. Rayleigh scattering is strongly wavelength dependent as the scattering intensity is inversely proportional to the 4^{th} power of wavelength.

The detailed derivation for Rayleigh scattering formulation can be found in light scattering literature [17] [18]. The Rayleigh scattering criteria is $x \ll 1$ and $|N|x \ll 1$, where N is the refractive index of particle, which is defined as:

$$N = N_r - iN_i \quad (3.2),$$

where N_r is the real part (accounting for refraction) and N_i the imaginary part (attenuation due to absorption). For low loss dielectrics, N_i approaches 0.

For Rayleigh scattering, the physical interpretation of the scattering criteria is $x<<1$ and $|N|x<<1$, is that, the particle is illuminated by a uniform electric field at any instance of time.

The formulation is for Rayleigh and Mie scattering is performed in a spherical coordinated system as seen in Fig. 3.4.

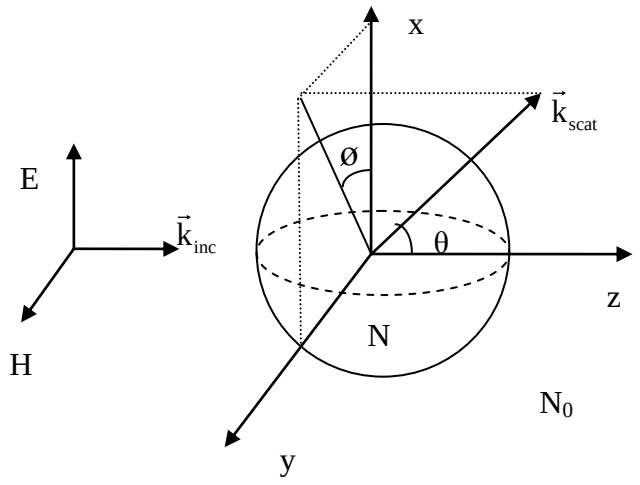

Figure 3.4: Spherical coordinate system.

Taking the polar angle θ to be the angle between incident beam and scattered beam, the scattered phase function, P(θ), is the angular distribution of scattered light intensity and is given by [16] [19]:

$$P(\theta) = \frac{\lambda^2}{8\pi^2}\left(\frac{\pi^2 D_p}{\lambda}\right)^6 \left|\frac{m^2 - 1}{m^2 + 2}\right| \left(1 + \cos^2(\theta)\right) I_o \quad (3.3),$$

where I_o is the incident light intensity, D the particle diameter, and $m = N / N_o$ the refractive index ratio of particle to surrounding medium. While Rayleigh scattering is uniformly distributed, Mie scattering has a stronger forward scattering component.

3.2 Inelastic Light Scattering

The scattering is termed inelastic, when wavelength of the scattered light is different from the wavelength of incident light. The three main types are: (a) Brillouin scattering, (b) Raman scattering, and (c) fluorescence. In these scatterings, if the scattered light has lower energy than the incident light, the shift is called the Stokes shift, if the scattered light has higher energy than the incident light, then the shift is called anti-Stokes shift. Here, we are interested in the fluorescence phenomenon.

3.2.1 Fluorescence

When electrons return from excited state to ground state, they emit photons. This process is called luminescence and has two types [20]: (a) fluorescence, and (b) phosphorescence.

There are two types of excited states, singlet and triplet. In singlet state, the electron spin of the electron is opposite to that of electron in ground state and these electrons are said to be paired. In the triplet state the spin is the same, and therefore the spin state of the electrons is unpaired. The emission when an electron returns from singlet state is called fluorescence. The emission when an electron returns from triplet state is called phosphorescence. The fluorescence lifetime is around 10 ns, whereas phosphorescence is a slow process having a lifetime from milliseconds to seconds. The two phenomena are shown in an energy level diagram called Jablonski diagram (Fig. 3.5).

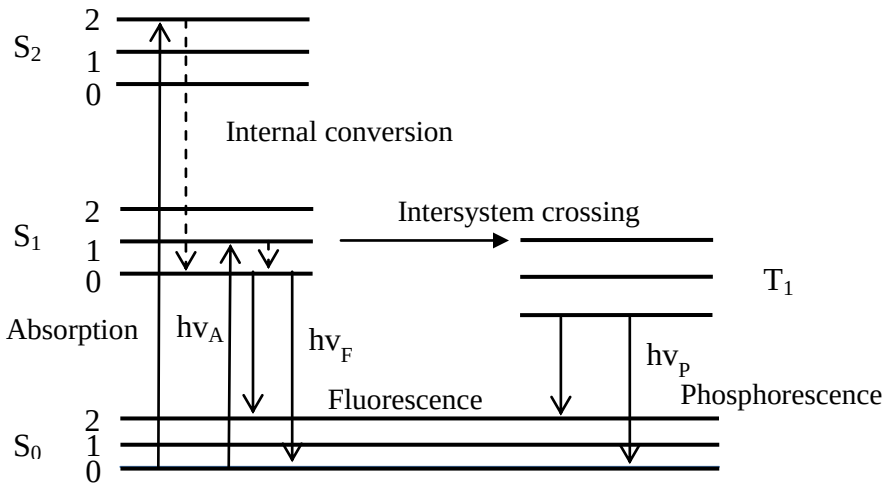

Figure 3.5: Jablonski diagram.

In Fig. 3.5, S_0, S_1, S_2 depict the singlet electronic states, and the energy lines within them represent the vibrational levels. When electrons are excited to upper energy states, they relax to lowest vibrational state of S_1, this happens very rapidly taking around picoseconds and the process is called internal conversion. Fluorescence usually takes places from the thermally equilibrated excited state. T_1 represent the triplet state, and the emission from these states is shifted to longer wavelength compared to fluorescence.

With fluorescence the shifts in wavelength are Stoke shifts. So there is energy loss between excitation and emission. The energy is lost during relaxing to lower vibrational level. The emission spectrum of fluorescence is independent of the exciting wavelength. The excess energy is released during the fluorophore relaxing to lowest vibrational level. The fluorescence is spectrally represented as emission spectra. The calculated fluorescence spectrum of Rhodamine 6G is shown in Fig.3.6.

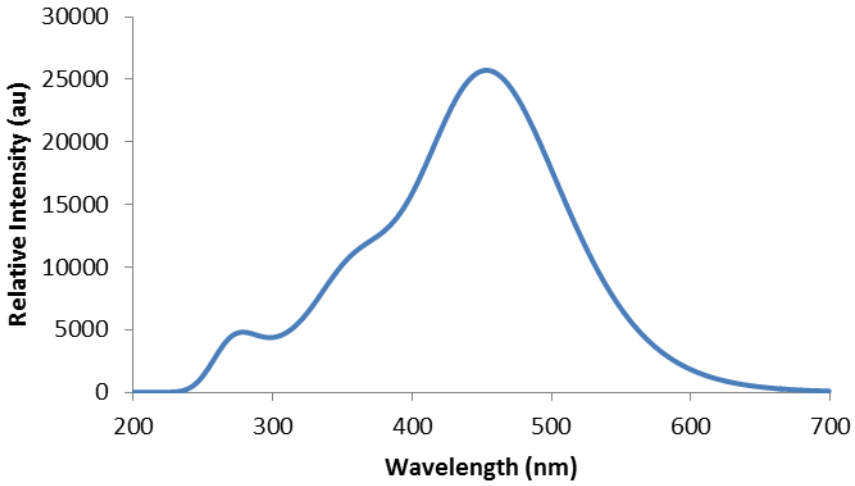

Figure 3.6: Simulation of fluorescence spectra of Rhodamine 6G in gas phase.

Fluorescence quantum yield, Φ_F, is the parameter used for finding the efficiency of the fluorescence process. Φ_F is the ratio of photons absorbed to photons emitted in fluorescence process [21].

3.3 Medium Properties that affect scattering

Rayleigh scattering is a simple approximation, which works well for the gases [22]. Rayleigh's theory ignores interaction between molecules, and assumes molecular dipole scattering independent of other molecules. In the Rayleigh regime, the overall scattered intensity is the product of the intensity per scatterer, and the number of scatterers.

In liquids, the molecules do not scatter independently. Liquid is an optically dense medium. Separation between molecules is considerably less than the wavelength of incident light, typically 2-3Å [15]. So the molecules are also acted on by the secondary field of other molecules besides the incident light.

Scattering arises due to the inhomogeneity in the dielectric constant of the medium [23]. In optically dense media scattering occurs due to the optical inhomogeneities resulting from the density fluctuations. The density fluctuations occur as the number of molecules in a given volume is same only on average, and will vary instantaneously and spatially [24]. These inhomogeneities will cause a fluctuation in the dielectric constant of the medium resulting in scattering. The intensity of the scattered light depends on the magnitude of the fluctuation in dielectric constant. Another type of fluctuation is the orientational fluctuation [15]. In liquid crystal molecules, in nematic phase, the molecules are aligned along a common axis. The molecule orientation can change both temporarily and spatially. The fluctuations lead to change in the dielectric tensor, thus scattering light [23].

3.3.1 Transparent Fluids

In the transparent mediums, light scattering still exists. The scattering is due fluctuations in the density of the medium. Even if macroscopically the medium is homogeneous, however, on a very small volume compared to wavelength of light, the number of molecules will fluctuate due to motion of molecules. This will result in change in dielectric constant on a small scale. The fluctuation is in very small size scale compared to the wavelength of incident light, and is called Rayleigh scattering [25].

For dense media, the thermodynamic theory of fluctuations can be used to obtain a light scattering formula, which can be expressed as [26]:

$$R = \frac{r^2 I_u(\theta)}{I_{ou}} = \left(\frac{\pi^2}{2\lambda^4{}_o}\right)\rho_o\left(\frac{\partial\varepsilon_{opt}}{\partial\rho_o}\right)^2_T\left(1+\cos^2\theta\right)L(h) \qquad (3.4),$$

where R is called the Rayleigh ratio, r the distance from the sample to the detector, I_u the intensity of the unpolarized light scattered per unit solid angle per unit sample volume, θ the scattering angle, I_{ou} the intensity of the unpolarized incident light, λ_o the wavelength of light in vacuum, ρ_o the number of particles per unit volume, ε_{opt} the dielectric constant at the frequency of the scattered light, and L(h) a quantity, which describes the effect of intermolecular interference, and the factor $\left(1+\cos^2\theta\right)$ accounts for the unpolarized incident light.

In our experiments, the transparent fluid used is ethanol. The chemical formula of ethanol is C_2H_5OH. The product is manufactured by Merck KGaA, Darmstadt, Germany. As already stated, the scattering is dependent on the change in the index of refraction of the material, and the volume in which, there are such changes. Ethanol molecules are small molecules. They are not much polarizable. Refractive index of ethanol is 1.36 in the visible range [27] [28]. Ethanol in solutions is homogenous, so there is not much scattering observed during experiments.

3.3.2 Turbid Fluid

In turbid media, the refractive index changes throughout the medium. Nematic liquid crystals (NLCs) act as turbid fluids [29]. This turbidity leads to strong scattering [30] [31]. The cause of this turbidity is the orientational fluctuations [32]. Scattering from NLCs is about 10^3 to 10^6 greater than a typical fluid [33]

The liquid crystal, we chose is 4-Cyano-4'-pentylbiphenyl, is a widely used nematic liquid crystal, and is known by the name of 5CB, and has the chemical formula $C_{18}H_{19}N$. Its transition from nematic phase to isotropic phase is 35.17 $^\circ$C. The nematic range of the 5CB is 18 – 35°C [34] [35]. 5CB molecule is rod like, 20 Å long and 5 Å wide [36]. In our work, we chose 5CB as

nematic liquid crystals as strong scatterers, and 5CB has nematic phase around room temperature. 5CB due to its rod–like shape moreover has different polarizabilities in different directions. 5CB forms a liquid crystal in which, the molecules are all aligned in the same direction, called the director, over long distance scales (Fig. 3.7) [37] [38]. There are bigger changes in index over longer distances resulting in increased scattering.

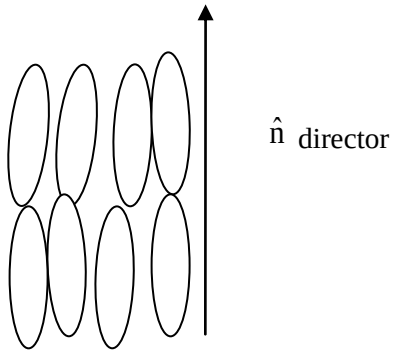

Figure 3.7: Nematic liquid crystal (NLC) representation.

3.4 Absorption

As already discussed in chapter 2, when light with energy, greater than bandgap energy, falls on the semiconductor material, incident light can get absorbed. We say that, the photon has been annihilated. The energy in the process is absorbed by the electron in valence band and jumps to the conduction band. We also mentioned, there is cutoff wavelength corresponding to the minimum energy required. The material acts as transparent to the longer wavelengths than this cutoff wavelength (Eq.2. 3).

3.4.1 Absorption Coefficient

Absorption coefficient, α, is an important term, when selecting materials for photodetection. The absorption coefficient $\alpha(cm^{-1})$ is related to N_i as:

$$\alpha = \frac{4\pi N_i}{\lambda} \quad (3.5),$$

The absorption coefficient α determines the distance light can travel in a material before being absorbed. The absorption coefficient α is different for different materials, and depends on the wavelength of incident light as well (Eq. 3.5). If a material has low absorption coefficient, its light absorption would be poor, and if the sample is thin enough, it might act as transparent for that wavelength. The penetration depth is given by the reciprocal of the absorption coefficient. Fig. 3.8 gives the absorption coefficients variation with wavelength for various semiconductors.

We are basically interested in silicon, whose cutoff wavelength is taken to be 1100 nm, corresponding to bandgap energy of 1.12 eV [7][39][40] [41]. Therefore, silicon photodetectors work in the visible and the near-IR range. From Fig. 18, it can be seen that the absorption coefficient of silicon is one to two order less in magnitude compared to some of the other materials, so the silicon detectors have to be built thicker than other semiconductor photodetectors.

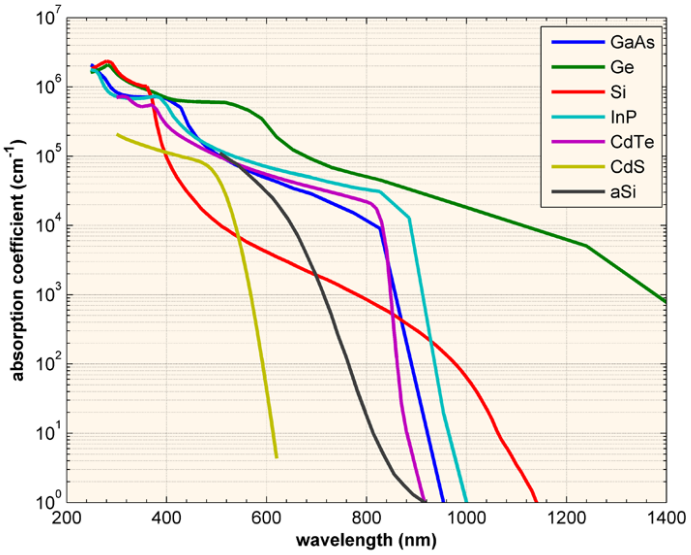

Figure 3.8: Absorption coefficient of semiconductors [42].

3.4.2 Beer-Lambert Law

The Beer-Lambert law helps in determining the attenuation in intensity of light, after passing through the absorbing medium (fig. 3.9). The Beer-Lambert law is expressed as [43]:

$$A = -\log_{10}\frac{P}{P_o} = abc \qquad (3.6),$$

where A is the absorbance, P the radiant power, P_o the incident power, a the absorptivity with units of L mol^{-1} cm^{-1}, b the length of the beam in the absorbing medium, and c the concentration of absorbing sample with units of mol L^{-1}. Absorbance is also referred to as optical density (OD) and is unit less. Absorptivity is the measure of the probability of an electronic transition. Absorptivity tells how strongly light will be absorbed at given wavelength. It is also called molar absorption coefficient, and molar extinction coefficient.

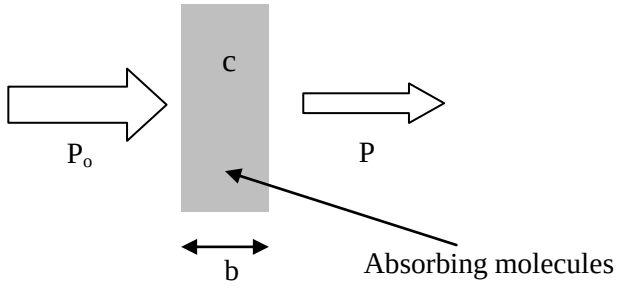

Figure 3.9: Light transmission through an absorbing medium.

The limitation of Beer's law is that it ignores scattering, so is not appropriate for scattering materials [44]. It has to be modified to account for the scattering and increased optical path way within the medium. Now if the media exhibits scattering as well as absorbance and the parameter measured in this situation is called extinction [15]. Extinction coefficient $\alpha_{extinction}$ is the sum of absorption and scattering coefficients, $\alpha_{absorption}$ and $\alpha_{scattering}$, respectively.

$$\alpha_{extinction} = \alpha_{absorption} + \alpha_{scattering} \quad (3.7).$$

Chapter 4

PHOTODETECTOR IN SCATTERING MEDIA

In this work, we observed enhanced photodetection by immersing photodiodes in liquid environment. We prepared various types of liquid environment to create elastic and inelastic light scattering conditions by using ethanol, 5CB nematic liquid crystal, Rhodamine 640 perchlorate laser dye with ethanol solution, and Rhodamine 640 perchlorate laser dye solution with the 5CB liquid crystal.

Ethanol and liquid crystal fluids were used for elastic light scattering, whereas Rhodamine 640 perchlorate laser dye mixture was used to produce inelastic light scattering. To test the geometric enhancement factors of the photodiodes, we devised a simple measurement setup having a green laser excitation for the fluid environments.

We characterized the electrical response of a conventional flat surface photodiode and a spherical shaped photodiode for tomography and spatial positioning. The spherical silicon photodiodes were manufactured by Kyosemi Corporation and Sphelar Power Corporation and named as Sphelar® [45].

Our results indicate that spherical photodiodes benefit from omnidirectionality and perform better than the conventional planar photodiodes.

4.1 Sphelar® Photodiode

Sphelar® photodiode used in this study is 1.8 mm in diameter and shaped as a sphere. The photodiode is doped p type in the core and doped n type on the surface to form a spherical shaped p-n junction (fig. 4.1). Electrical connections are formed by aluminum electrode connected to p doped core and silver electrode connected to the n doped surface [46].

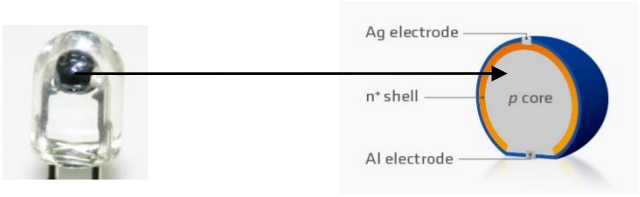

Figure 4.1: (a) Image and b) cross section of the Sphelar® photodiode.

4.2 Flat Photodiode

The conventional flat photodiode is composed of silicon and forms a planar surface with dimensions of 3 mm by 3 mm (fig. 4.2). This type of photodiode is used heavily in the electronics and photonics applications.

Figure 4.2: Flat silicon photodiode.

4.3 Electrical Characterization

The IV setup used to characterize our photodiodes is shown in fig. 4.3. Two programmable dc power supplies are used to apply forward and reverse bias to the photodiodes. Power supplies are connected to computer via serial ports. An oscilloscope is used to measure the voltage and is connected to the computer via GPIB interface. An amperemeter is connected to computer via USB port. LabVIEW® interface is designed for control and data acquisition for I-V measurements. Fig. 4.4 shows the IV measurement of Sphelar® sphere in the dark. Fig. 4.5 shows the IV curve of flat silicon photodiode in the dark.

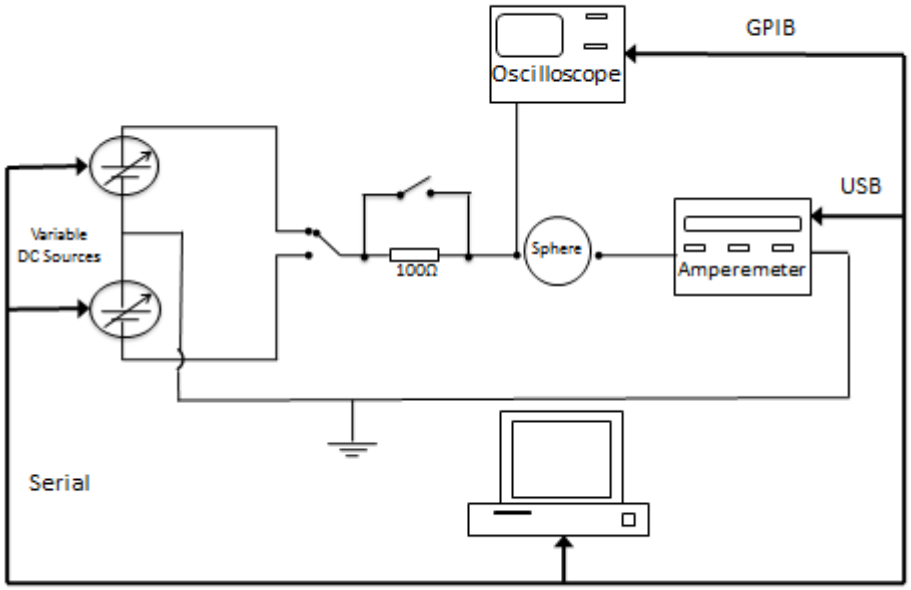

Figure 4.3: Electrical I-V measurement setup.

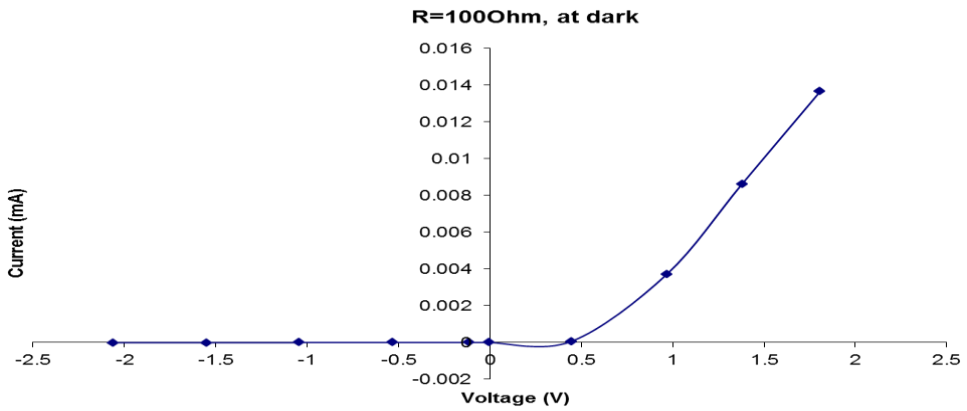

Figure 4.4: I-V curve of the Sphelar® spherical photodiode.

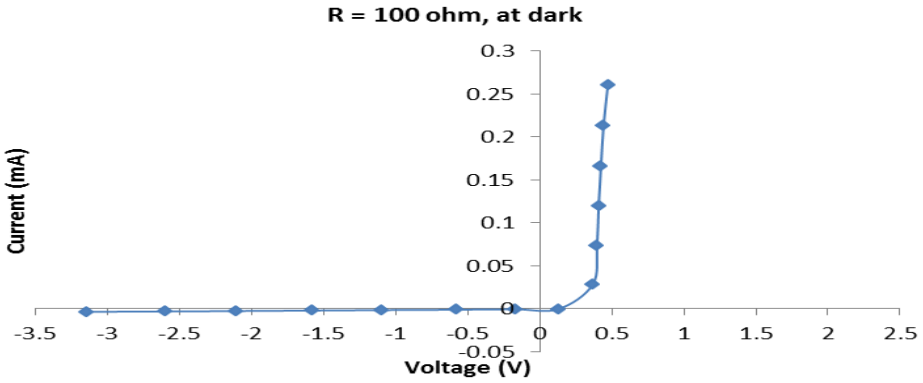

Figure 4.5: Flat Silicon Photodiode I-V curve.

4.4 Rhodamine 640 perchlorate laser dye

Laser dyes are organic chemicals. Rhodamine 640 per chlorate (R640) has a synonym Rhodamine 101. The difference is that the anion in Rhodamine 101 is a chloride [47]. The laser dye is an Exciton product. The chemical formula of R640 is $C_{32}H_{31}N_2O_3.ClO_4$. The molecular

weight is 591.05. The dye appears to be dark green crystals with bronze sheen [48]. When excited by green laser (532 nm), the dye fluoresces in the 590-680 nm range [49].

4.5 Experimental Setup

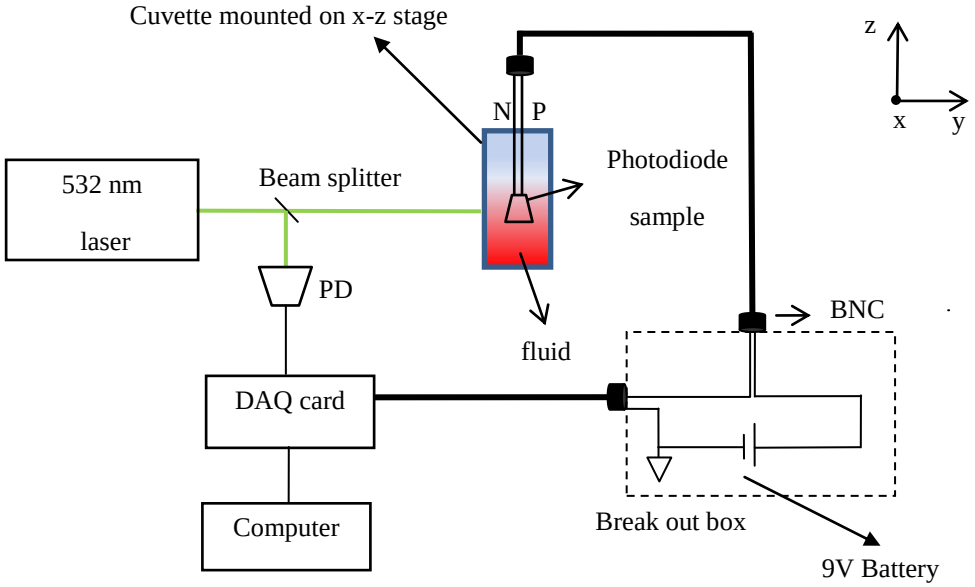

Figure 4.6: Schematic of the experimental setup.

The experimental setup is shown in fig. 4.6. A diode pumped solid state (DPSS) green laser (8mW@ 532 nm) was used. A beam splitter is placed between the laser and a cuvette to direct fraction of light to a si Photodiode. The cuvette is mounted on a x-z stage to scan the laser in horizontal and vertical directions. Plastic cuvettes with 1 cm width are used. The solutions used were 3 ml in volume. The photodiodes were immersed in the cuvette, with one end connection connected to a break out box using BNC connectors. A 9 V battery is connected to the break out

box to reverse bias the photodiode in photoconductive mode. The 3rd connection of break out box leads to the Data acquisition card (DAQ). DAQ card is connected to the computer. A LabVIEW® interface is designed for control and data acquisition.

4.6 Sign convention for plotting results

Fig. 4.7 gives the sign convention used during scanning. Initially the sample position was located and given a (0,0) coordinates. Throughout the experiment laser position was kept same and sample was moved along x-z axes. The measurements taken were horizontally on-sample and 2 mm horizontally above and below samples, also vertically on-sample and 2 mm vertically right and left of the sample.

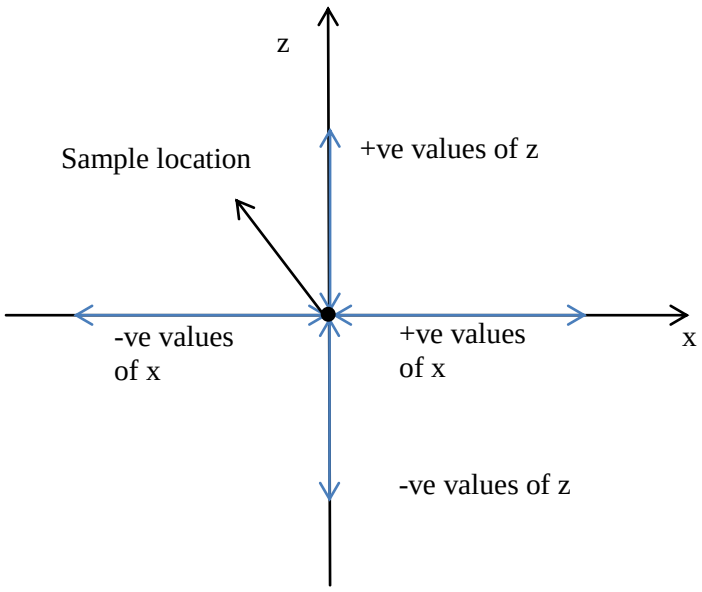

Figure 4.7: Sign convention for scanning the response of the photodetectors.

4.7 Spatial Tomography Results

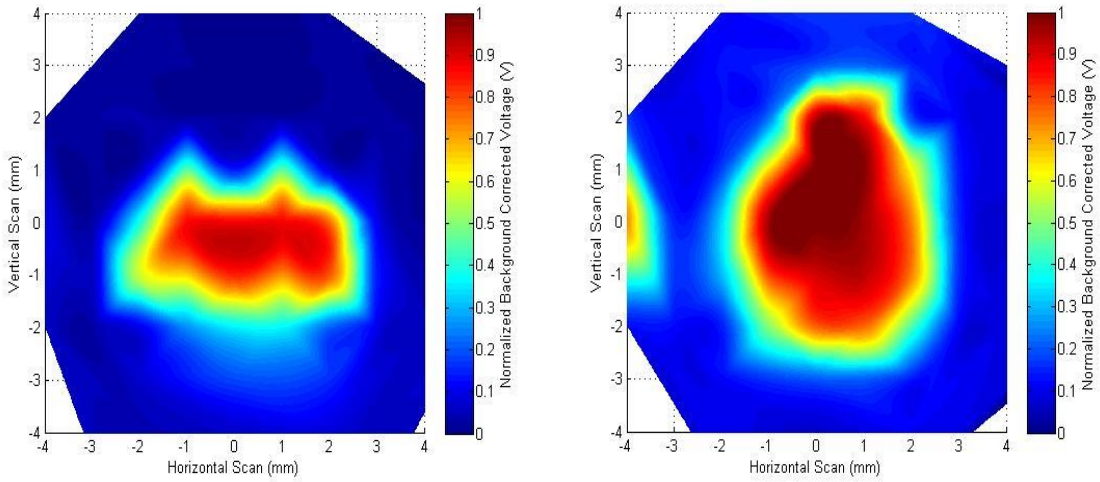

(a) (b)

Figure 4.8 (a) Flat and (b) Sphelar® photodiode in ethanol.

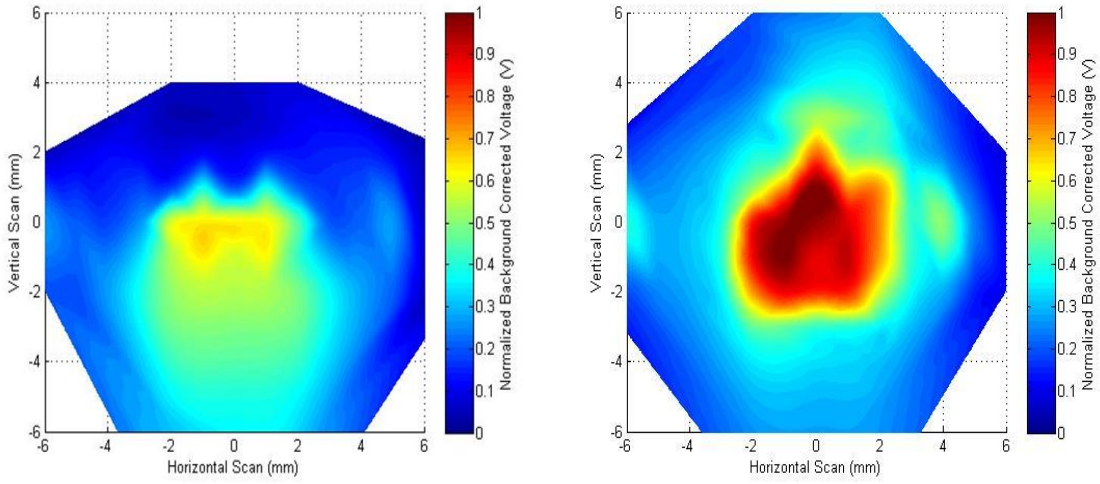

(a) (b)

Figure 4.9 (a) Flat and (b) Sphelar® photodiode in 0.1 mM solution of R640/ ethanol.

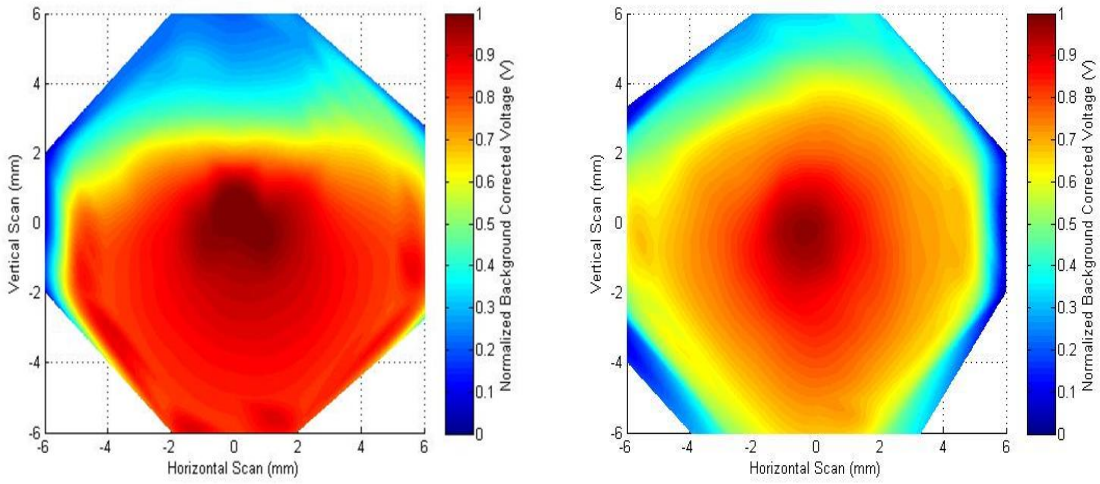

(a) (b)

Figure 4.10 (a) Flat and (b) Sphelar® photodiode in 5CB LC.

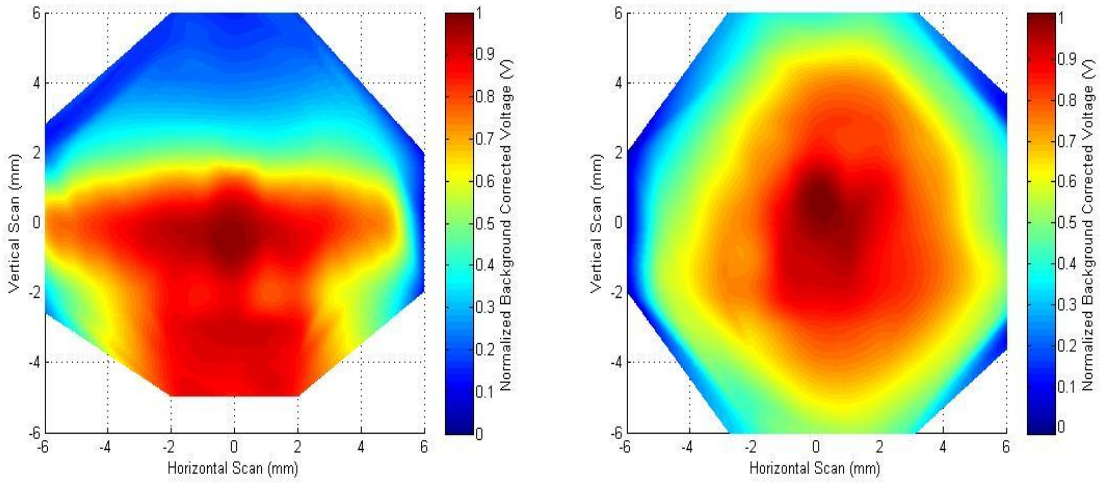

(a) (b)

Figure 4.11 (a) Flat and (b) Sphelar® photodiode in 0.1 mM solution of R640/ 5CB LC.

The two samples used are Sphelar® photodiode and the flat photodiode. The plane of the photodiode was along x-y axes facing the negative z-axis. On-sample position was located by first scanning horizontally and vertically near the sample region and locating (x,z) points with maximum voltage reading. Measurements were made with the step size of 1 mm. The stages used were manual linear translation stages with travel range of 25 mm capability. For plotting, the voltages were averaged. The background was measured and the readings were corrected for the background and these background corrected voltages were plotted versus relative (x, z) location position of the sample with respect to laser.

Fig. 4.8-11 are Matlab ® plots of the x-z scans in the four solutions, we had. These plots have three data sets for horizontal scans, and three data sets for the vertical scans, and then cubic interpolation with 0.01 mm step size was performed. Fig. 4.8-11 represents effect of geometry of our samples on the collection of light. Fig. 4.8 is the comparison of photodiodes immersed in ethanol. Flat photodiode response is more directional compared to the Sphelar® photodiode response, which was expected as spherical geometry is able to collect light from all directions. Flat photodiode‘s response is better in the –ve z-axis region compared to +ve z axis region due to the orientation of the sample, whereas Sphelar® photodiode response is not affected by relative position with respect to the laser. This pattern is present in all of the subsequent plots with flat photodiode outperforming Sphelar® photodiode in the –ve z region. One of the reasons is the flat photodiode used had surface area of 3 x 3 mm, whereas Sphelar® photodiode had 1.8 mm diameter, so larger flat photodiode surface area was being illuminated.

In ethanol and ethanol laser dye solution, Sphelar® photodiode records higher maximum voltage, where as in LC and 5CB/ LC solution, the maximum voltage is the same. Overall Sphelar®

photodiode appears to outperform flat photodiode in its ability to collect light from different directions. Its performance is better in transparent solution and in scattering liquids, flat photodiode is slightly better in negative z region largely due to surface area advantage.

4.7.1 Effect of Solutions on the Sphelar® photodiode

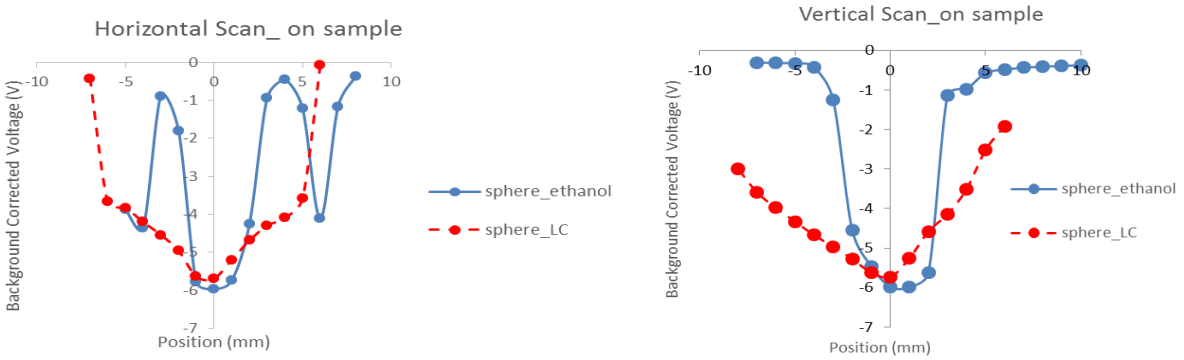

(a) (b)

Figure 4.12 (a) horizontal and, (b) vertical scan of Sphelar® in ethanol vs. 5CB LC.

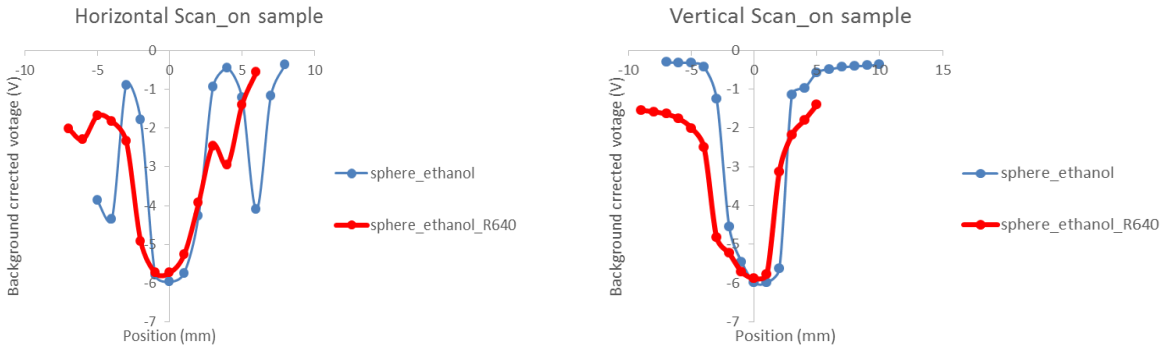

(a) (b)

Figure 4.13 (a) horizontal and, (b) vertical scan of Sphelar® in pure vs. 0.1 mM R640/ethanol.

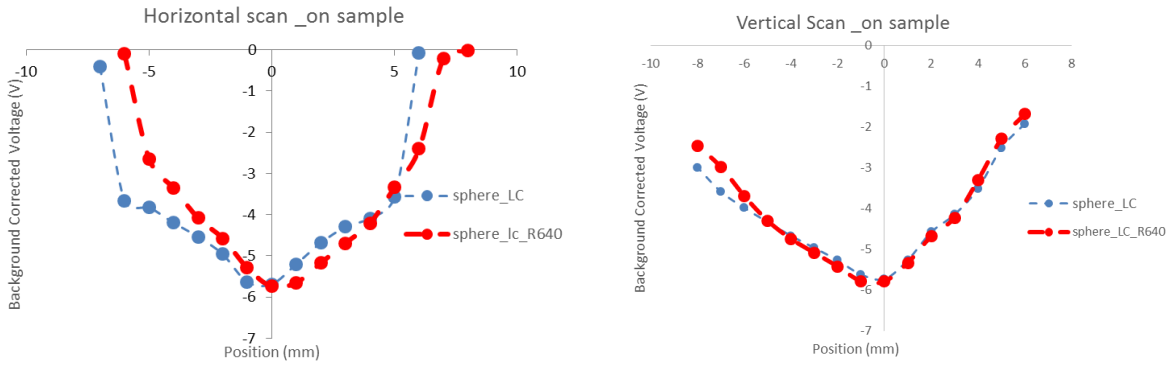

(a) (b)

Figure 4.14 (a) horizontal, and (b) vertical scan of Sphelar® in pure vs. 0.1 mM R640/5CB LC.

In Fig. 4.12-14, the sample used is Sphelar® photodiode and comparison is being made between different solutions' effect on the photodetection. Figure 4.12 is the comparison between ethanol and LC, ethanol being a weakly scattering solution, because of its transparency and 5CB a strongly scattering solution in its nematic phase. Fig. 4.12 (a) represents horizontal scan and Fig. 4.12 (b) represents vertical scan for the Sphelar® photodiode. This is the case of elastic light scattering comparison and as can be seen, collection of light from 5CB LC is far better than ethanol. In 4.12 (a), the voltage increases at the end positions, because of strong reflections observed, when laser was hitting the edge of the cuvette.

Fig 4.13 draws comparison between ethanol and 0.1 mM R640/ethanol solution for the Sphelar® photodiode. R640/ethanol solution fluoresces, when hit by the green laser, so there is inelastic scattering present in the solution. From the plots, it can be seen that, the area under the curve has increased in the case of fluorescent solution compared to just elastic light scattering present in ethanol solution.

Fig 4.14 draws comparison between 5CB LC and 0.1 mM R640/5CB LC solution for the Sphelar® photodiode. In this comparison, 5CB has elastic light scattering, whereas R640 induces fluorescence in the other solution. However the plots are similar, so fluorescence does not seem to enhance the scattering. Rhodamine 640 has a very high fluorescence quantum yield, reaching 100 percent [50], so for no noticeable difference in our results, one reason could be that, absorption is interfering with scattering.

We only used 0.1mM laser dye solution, so different dilutions must be used to see the impact of different concentration of our solutions on the absorption, as absorbance is related to concentration according to Lambert-Beer' law [51].

Also the fluorescence is influenced by the surrounding solvent medium [52] [53] [54]. For our case, it appears that, in ethanol as solvent, there is more scattering then in 5CB LC.

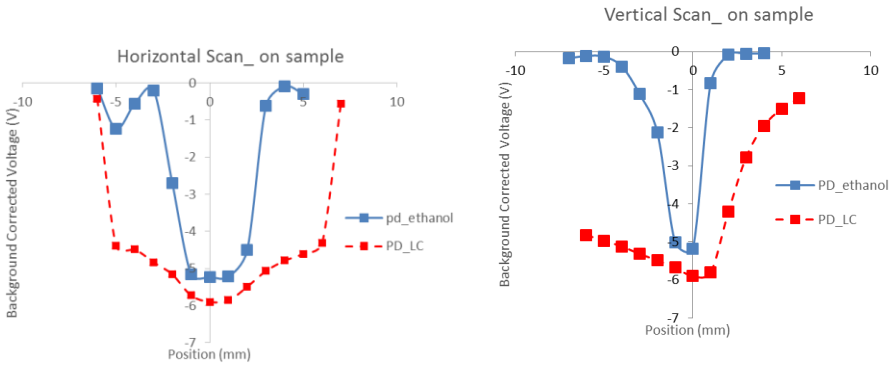

(a) (b)

Figure 4.15 (a) horizontal and, (b) vertical scan of flat PD in pure ethanol vs. pure 5CB LC.

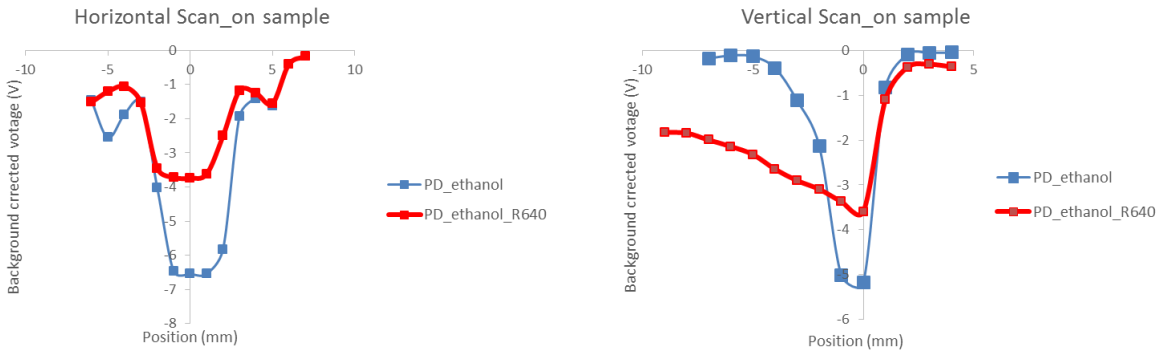

(a) (b)

Figure 4.16 (a) horizontal and, (b) vertical scan of flat PD in pure vs. 0.1 mM R640/ethanol.

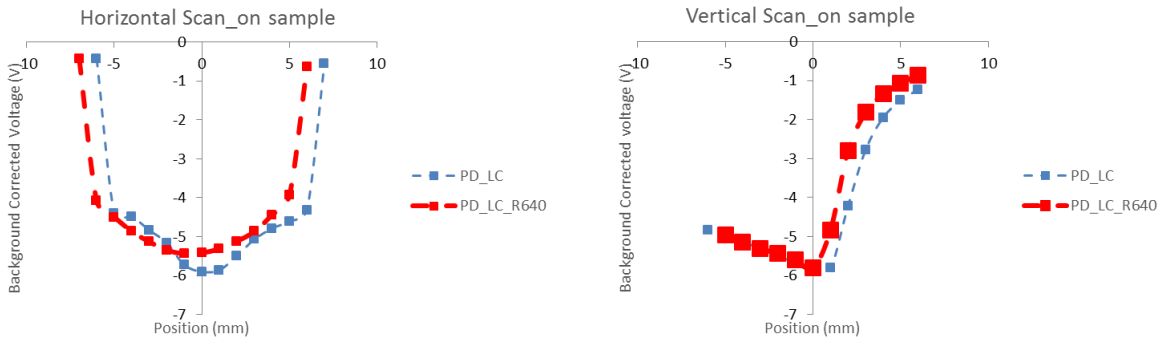

(a) (b)

Figure 4.17 (a) horizontal and, (b) vertical scan of flat PD in pure vs. 0.1 mM R640/5CB LC.

In Fig. 4.15-17, the sample used is the flat photodiode and comparison is being made between different solutions' effect on the photodetection. Fig. 4.15 gives the comparison for strong scattering medium 5CB liquid crystal versus weak scattering medium ethanol. Like the Sphelar® photodiode case area under the curve for the liquid crystal is large. Horizontal scan results of flat photodiode voltage for 0.1 mM R640/ethanol are very low compared to ethanol. Vertical scan

results, however, show higher voltages. The results for the photodetection cases in 5CB LC and 0.1 mM R640/5CB LC are same, just like the results were for the Sphelar® photodiode. So fluorescence is not able to add to scattering of nematic liquid crystal, with the concentrations, we are using.

Chapter 5

CONCLUSIONS

Elastic and inelastic light scattering based photodetection in amorphous and crystalline liquids is presented. The experimental setup and results are discussed together with the theory of the photodetectors, and the light matter interactions occurring in our experiment. Photodetection was done in photoconductive mode with two different geometries: (a) flat photodiode, and (b) Sphelar® photodiode. Solutions used were ethanol, 0.1 mM R640/ ethanol solution, 5CB LC, and 0.1 mM R640/ 5CB LC solution. Ethanol was used as a weak elastic light scattering medium, 5CB LC as a strong elastic light scattering medium, and R640 laser dye was used to produce fluorescence, which is inelastic light scattering.

The geometric advantage of spherical photodiode was obvious, we were able to see strong scattering from 5CB LC as well. The increase in photodetection in presence of fluorescence was there in ethanol, but not, when mixed with LC.

We think results can be further improved by decreasing the step size, 1 mm step size seemed too large. Also, more experiments need to be conducted to average out the results; the results shown here are from a single experiment only. Also to observe the role of the laser dye, we need to change the dilutions of the solutions. Automating the scanning of the setup can also increase resolution and eliminate human error.

Elastic and inelastic scattering enhanced spherical and flat silicon photodiodes in amorphous and crystalline liquids, can find application industrial areas, where liquids sensors are used, such as automotive, aeronautics, medicine, defense, security, and civil engineering.

VITA

Muhammad Hamza Humayun received his B.Sc. degree from Department of Electrical Engineering, University of Engineering & Technology, Lahore, Pakistan in 2007. He later worked in service sector and different academic institutions in Lahore until 2013. He was then selected for Higher Education Commission (HEC) Pakistan's Universities of Engineering, Science & Technology of Pakistan (UESTP) program for studies abroad and joined Koç University, Istanbul, Turkey. He joined M. Sc. in Optoelectronics and Photonics Engineering program at Koç University in 2013. For his M. Sc. degree thesis he worked on “Elastic and Inelastic Scattering Enhanced Spherical and Rectangular Silicon Photodiodes in Amorphous and Crystalline Liquids”.

BIBLIOGRAPHY

[1] T.C. Chiang and F. Seitz. "Photoemission spectroscopy in solids," *Annalen der Physics* (Leipzig), vol. 10, no. 1-2, pp. 61–74, 2001.

[2] P.R. Norton, “Photodetectors,” in Handbook of Optics, 2nd ed., M. Bass, Ed. McGraw-Hill, 1995.

[3] A.M. Joshi and G.H. Olsen, “Photodetection,” in Handbook of Optics, 2nd ed., M. Bass, Ed. McGraw-Hill, 1995.

[4] F.L. Pedrotti and L.S. Pedrotti, Introduction to Optics, 2nd ed. Prentice-Hall, 1993.

[5] B.H. Bransden and C.J. Joachain, Quantum Mechanics, 2nd ed. Pearson, 2000.

[6] M.A. Omar, "Elementary Solid State Physics", Addison-Wesley, 1975.

[7] S.M. Sze, Physics of Semiconductor Devices, 2nd ed. Wiley, 1998.

[8] J-M. Liu, Photonic Devices. Cambridge University Press, 2009.

[9] B.E.A. Saleh and M. C. Teich, Fundamentals of Photonics, 2nd ed. Wiley, 2007.

[10] F. J. Cox, Fundamentals of linear electronics: integrated and discrete. Cengage Learning, 2001.

[11] L.I. Berger, Semiconductor Materials, CRC Press, 1997.

[12] Hamamatsu Photonics KK, Opto-Semiconductor Handbook, Solid State Division, Hamamatsu City, Japan 1999.

[13] J.E. Bowers and Y.G . Wey, “High-Speed Photodetectors,” in Handbook of optics, 2nd ed., Michael Bass, Ed. McGraw-Hill, 1995.

[14] J. Flammer, M. Mozaffarieh, and H. Bebie, “The Interaction Between Light and Matter,” in Basic Sciences in Ophthalmology, Springer Verlag, pp. 21–39, 2013.

[15] C.F. Bohren and D.R. Huffman, Absorption and scattering of light by small particles. Wiley, 1998.

[16] J.H. Seinfeld and S.N. Pandis, Atmospheric chemistry and physics from air pollution to climate change. Wiley, 2006.

[17] M. Kerker, The Scattering of Light and Other Electromagnetic Radiation, Academic Press, 1969.

[18] H. C. van de Hulst, Light scattering by small particles. John Wiley & Sons, 1957, (Dover, 1981).

[19] V.V. Vysotskii, O.Y. Uryupina, A.V. Gusel’nikova, and V.I. Roldugin, “On the feasibility of determining nanoparticle concentration by the dynamic light scattering method,” *Colloid Journal*, vol. 71, no. 6, pp. 739–744, 2009.

[20] J. R. Lakowicz, Principles of Fluorescence Spectroscopy. Springer US, 1983.

[21] C. Würth, M. Grabolle, J. Pauli, M. Spieles, and U. Resch-Genger , "Relative and absolute determination of fluorescence quantum yields of transparent samples." *Nature Protocols*, vol. 8, no. 8, pp. 1535-1550, 2013.

[22] W. L. Eberhard "Correct equations and common approximations for calculating Rayleigh scatter in pure gases and mixtures and evaluation of differences," *Applied Optics*, vol. 49, no.7, pp.1116-1130, 2010.

[23] J.T. Ho, "Light scattering and quasi-elastic spectroscopy," in Liquid crystals: experimental study of physical properties and phase transitions, S. Kumar, Ed. Cambridge University Press, 2001.

[24] L.D. Barron, Molecular light scattering and optical activity, Cambridge University Press, 2nd ed., 2009.

[25] G.S. He and S.H. Liu, Physics of nonlinear optics, vol. 216, World Scientific, 1999.

[26] B. Chu and P. W. Schmidt, "Light scattering from simple dense fluids," in Simple dense fluids, H.L. Frisch, Ed. Elsevier Science, 1968.

[27] C. Wohlfarth, "Refractive index of ethanol." Refractive Indices of Pure Liquids and Binary Liquid Mixtures (Supplement to III/38), Springer Verlag, 2008.

[28] S. Kedenburg, M. Vieweg, T. Gissibl, and H. Giessen, "Linear refractive index and absorption measurements of nonlinear optical liquids in the visible and near-infrared spectral region," *Optical Materials Express*, vol. 2, no. 11, pp. 1588-1611, 2012.

[29] R.S. Porter and J.F. Johnson, "Order and Flow of Liquid Crystals: The Nematic Mesophase," *Journal of Applied Physics*, vol. 34, no. 1, p. 51, 1963.

[30] H. Stark and T.C. Lubensky, “Multiple light scattering in nematic liquid crystals,” *Physical Review Letters*, vol. 77, no. 11, p. 2229, 1996.

[31] S. Gottardo, S. Cavalieri, O. Yaroshchuk, and D.S. Wiersma, “Quasi-Two-Dimensional Diffusive Random Laser Action,” *Physical Review Letters*, vol. 93, no. 26, 263901, 2004.

[32] G. Vertogen and W.H. Jeu, Thermotropic liquid crystals, fundamentals, Springer Verlag, 1988.

[33] P.M. Chaikin and T.C. Lubensky, Principles of condensed matter physics, vol. 1, Cambridge University Press, 2000.

[34] S. Weiss and G. Ahlers, “Nematic–isotropic phase transition in turbulent thermal convection,” *Journal of Fluid Mechanics*, vol. 737, pp. 308–328, 2013.

[35] O.V. Yaroshchuk, Y.P. Piryatinskiĭ, L.A. Dolgov, T.V. Bidna, and D. Enke, “Fluorescence of the nematic liquid crystal 5CB in nanoporous glasses,” *Optics and Spectroscopy*, vol. 100, no. 3, pp. 394–399, 2006.

[36] W. Gwizdala and Z. Gburski, “Molecular Order And Dynamics Of 5cb Liquid Crystals In Confined Space–Computer Simulation,” *Task Quarterly*, Vol. 19, No. 1, pp. 35–64, 2015.

[37] P.P. Gaikwad and M.T. Desai, “Liquid Crystalline Phase & its Pharma Applications,” *International Journal of Pharma Research & Review*, vol. 2, no. 12, pp. 40–52, 2013.

[38] M.J. Stephen and J.P. Straley, "Physics of liquid crystals." *Reviews of Modern Physics*, vol. 46, no. 4, p. 617, 1974.

[39] H. Zimmermann, Integrated Silicon Optoelectronics. Springer Verlag, 2010.

[40] W.C. Dash and R. Newman, “Intrinsic optical absorption in single-crystal germanium and silicon at 77 K and 300 K,” *Physical Review*, vol. 99, no. 4, p. 1151, 1955.

[41] M.A. Green and M.J. Keevers, "Optical properties of intrinsic silicon at 300 K," *Progress in Photovoltaics: Research and Applications*, vol. 3, no.3, pp. 189-192, 1995.

[42] http://www.pveducation.org/pvcdrom/pn-junction/absorption-coefficient

[43] D.F. Swinehart, “The Beer-Lambert Law,” *Journal of Chemical Education*, vol. 39, no. 7, p. 333, 1962.

[44] S.A. Prahl, M. J. C. van Gemert, and A. J. Welch. "Determining the optical properties of turbid media by using the adding–doubling method," *Applied Optics*, vol. 32, no. 4, pp. 559-568, 1993.

[45] http://sphelarpower.com/

[46] J. Nakata, "Spherical cells promise to expand applications for solar power," *Asia Electronics Industry*, pp. 44-46, 2001.

[47] J.M. Kauffman, “Laser dye structures and synonyms,” *Applied Optics*, vol. 19, no. 20, pp. 3431–3435, 1980.

[48] http://www.exciton.com/pdfs/r640.pdf

[49] http://www.exciton.com/wavelength_chart.html

[50] T. Karstens and K. Kobs, "Rhodamine B and Rhodamine 101 as reference substances for fluorescence quantum yield measurements." *Journal of Physical Chemistry*, vol. 84, no. 14, pp. 1871-1872, 1980.

[51] S. Fery-Forgues and D. Lavabre, "Are fluorescence quantum yields so tricky to measure? A demonstration using familiar stationery products," *Journal of Chemical Education*, vol.76, no. 9, p. 1260, 1999.

[52] G. Jones, W.R. Jackson, C.Y. Choi, and W.R. Bergmark, "Solvent effects on emission yield and lifetime for Coumarin laser dyes. Requirements for a rotatory decay mechanism," *Journal of Physical Chemistry*, vol. 89, no. 2, pp. 294-300, 1985.

[53] D. Magde, G.E. Rojas, and P.G. Seybold. "Solvent dependence of the fluorescence lifetimes of Xanthene dyes," *Photochemistry and Photobiology*, vol. 70, pp. 737-744, 1999.

[54] K.G. Casey and E.L. Quitevis. "Effect of solvent polarity on nonradiative processes in Xanthene dyes: Rhodamine B in normal alcohols." *Journal of Physical Chemistry*, vol. 92, no. 23, pp. 6590-6594, 1988.